Scientia Iranica E (2017) 24(5), 2605–2622

Sharif University of Technology
Scientia Iranica
Transactions E: Industrial Engineering
www.scientiairanica.com

Maximum multivariate exponentially weighted moving average and maximum multivariate cumulative sum control charts for simultaneous monitoring of mean and variability of multivariate multiple linear regression profiles

R. Ghashghaei and A. Amiri*

Department of Industrial Engineering, Faculty of Engineering, Shahed University, Tehran, Iran.

Received 24 November 2015; received in revised form 15 March 2016; accepted 13 August 2016

KEYWORDS
Multivariate multiple linear regression profiles;
Simultaneous monitoring;
Phase II;
Diagnosis aids.

Abstract. In some applications, quality of product or performance of a process is described by some functional relationships among some variables known as multivariate linear profile in the literature. In this paper, we propose Max-MEWMA and Max-MCUSUM control charts for simultaneous monitoring of mean vector and covariance matrix in multivariate multiple linear regression profiles in Phase II. The proposed control charts also have the ability to diagnose whether the location or variation of the process is responsible for out-of-control signal. The performance of the proposed control charts is compared with that of the existing method through Monte-Carlo simulations. Finally, the applicability of the proposed control charts is illustrated using a real case of calibration application in the automotive industry.

1. Introduction

Sometimes, quality of a process or product in the industry and non-industry is characterized by a relationship between two or more variables, which is presented by a 'profile' in the literature. In different applications, simple linear regression, multiple linear or polynomial regression, or even more complicated models such as nonlinear regressions are used to model the quality of processes. The applications of profile monitoring in the literature have been introduced by several authors such as Kang and Albin [1], Mahmoud and Woodall [2], Woodall et al. [3], Wang and Tsung [4], Woodall [5], Zou et al. [6], and Amiri et al. [7]. A profile monitoring problem consists of two phases, including Phase I and Phase II. The purpose of Phase I monitoring is providing an analysis of the preliminary data for estimating the process parameters. The main purpose of Phase II profile monitoring is designing a control scheme to detect different out-of-control scenarios in the process parameters. Monitoring of different types of linear regression profiles, such as simple linear, multiple linear, and polynomial regression profiles, has been investigated by many researchers. Kang and Albin [1], Kim et al. [8], Zou et al. [6], Keshtelia et al. [9], Noorossana and Ayoubi [10], and Chuang et al. [11] have studied Phase II monitoring of simple linear profiles. Researchers such as Kang and Albin [1], Mahmoud and Woodall [2], Mahmoud et al. [12], and Chuang et al. [11] have considered monitoring of simple

*. *Corresponding author. Tel.: +98 21 51212023;*
E-mail addresses: r.qashqaei@shahed.ac.ir (R. Ghashghaei); amiri@shahed.ac.ir (A. Amiri)

doi: 10.24200/sci.2017.4385

linear profiles in Phase I. Multiple linear regression and polynomial profiles have been studied by Zou et al. [6], Kazemzadeh et al. [13,14], Amiri et al. [15], and Wang [16].

In some situations, quality of a process or a product can be effectively characterized by two or more multiple linear regression profiles in which response variables are correlated, referred to as multivariate multiple linear regression profiles [17]. Noorossana et al. [18] proposed three control chart schemes for Phase II monitoring of multivariate simple linear profiles. They also used the term Average Run Length (ARL) to evaluate the proposed control charts. Noorossana et al. [19] developed four control charts in Phase I for monitoring of multivariate multiple linear regression profiles. They compared the performance of the proposed control charts through simulation studies in terms of probability of a signal. Zhang et al. [20] developed a new modelling and monitoring framework for analysis of multiple linear profiles in Phase I. Their framework used the regression-adjustment method in the functional principal component analysis. Eyvazian et al. [21] suggested four control charts to monitor multivariate multiple linear regression profiles in Phase II. They evaluated the performance of the proposed control charts through simulation studies in terms of the ARL criterion. They also used a numerical example to assess the performance of the developed control charts. Amiri et al. [17] introduced a diagnosis method to identify the profiles and parameters responsible for out-of-control signal in multivariate multiple linear regression profiles in Phase II.

In addition to the problems noted above, practitioners are interested in developing some kinds of control charts which can monitor mean and variability of processes simultaneously. In fact, the quality engineers want to have a single control chart instead of two or more. In practice, the control charts for monitoring both process mean and variability should be implemented together because assignable causes can affect both of them. In recent years, joint monitoring of process mean and dispersion in both univariate and multivariate cases has been considered by some researchers. Simultaneous monitoring of the mean and variance in univariate process has been studied by Khoo et al. [22], Zhang et al. [23], Guh [24], Memar and Niaki [25], Teh et al. [26], Sheu et al. [27], Haq et al. [28], and Prajapati and Singh [29]. The simultaneous monitoring of multivariate process mean vector and covariance matrix has also been addressed by several authors. Chen et al. [30] proposed a control scheme called Max-EWMA for monitoring both mean and variance simultaneously. They performed a comparison analysis and found that their proposed control chart performed better than the combination of chi-square and |S| control charts when small shifts occurred in the process parameters. Cheng and Thaga [31] proposed Max-MCUSUM control chart to detect any changes in mean vector and covariance matrix simultaneously. Zhang et al. [32] proposed a new control chart (ELR control chart) based on the combination of Generalized Likelihood Ratio (GLR) test and the Exponentially Weighted Moving Average (EWMA) control chart for simultaneous monitoring of mean vector and covariance matrix in the multivariate process. Wang et al. [33] applied the generalized likelihood ratio test and the multivariate exponentially weighted moving covariance control chart to monitor the mean vector and the covariance matrix of a multivariate normal process, simultaneously. Other research for simultaneous monitoring of multivariate process consists of Khoo [34], Hawkins and Maboudou-Tchao [35], Ramos et al. [36], and Pirhooshyaran and Niaki [37]. For detailed information on simultaneous monitoring of the process location and dispersion, refer to the review paper provided by McCracken and Chakraborti [38].

According to the literature, in most of the control charts proposed for monitoring of multivariate multiple linear regression profiles, mean vector and covariance matrix are monitored with separate control charts. In addition, these control charts are unable to diagnose whether the location or the dispersion is responsible for out-of-control signal. In this paper, we propose two methods for simultaneous monitoring of mean vector and covariance matrix in multivariate multiple linear regression profiles. Moreover, the proposed control charts are able to diagnose whether location or dispersion is responsible for out-of-control signal. The performance of the proposed control charts is compared with ELRT control chart proposed by Eyvazian et al. [21] in Phase II in terms of Average Run Length (ARL) and Standard Deviation Run Length (SDRL). The structure of the rest of this paper is as follows: In Section 2, we express multivariate multiple linear regression profiles model. In Section 3, the ELRT control chart is described. In Section 4, the proposed control charts are expressed. In Section 5, diagnosing procedure is explained. In Section 6, the comparison analysis of the proposed control charts is provided through an illustrative example. In Section 7, the application of the proposed control charts is illustrated by a real dataset. Finally, our concluding remarks and future research are given in Section 8.

2. Model and Assumptions

Let us assume that for the kth random sample collected over time, we have n observations given as $(x_{1i}, x_{2i}, \ldots, x_{qi}, y_{1ik}, y_{2ik}, \ldots, y_{pik})$, $i = 1, 2, \ldots, n$ where p and q are the numbers of response variables and explanatory variables, respectively. When the process is in statistical control, the model that relates the response variables with explanatory variables is a multivariate multiple linear regression model and is given as follows [21]:

$$\mathbf{Y}_k = \mathbf{XB} + \mathbf{E}_k, \tag{1}$$

or equivalently:

$$\begin{bmatrix} y_{11k} & y_{12k} & \cdots & y_{1pk} \\ y_{21k} & y_{22k} & \cdots & y_{1pk} \\ \vdots & \vdots & \ddots & \vdots \\ y_{n1k} & y_{n2k} & \cdots & y_{npk} \end{bmatrix} = \begin{bmatrix} 1 & x_{11} & \dots & x_{1q} \\ 1 & x_{21} & \dots & x_{2q} \\ \vdots & \vdots & \ddots & \vdots \\ 1 & x_{n1} & \dots & x_{nq} \end{bmatrix} \begin{bmatrix} \beta_{01} & \beta_{02} & \dots & \beta_{0p} \\ \beta_{11} & \beta_{12} & \dots & \beta_{1p} \\ \vdots & \vdots & \ddots & \vdots \\ \beta_{q1} & \beta_{q1} & \dots & \beta_{qp} \end{bmatrix} + \begin{bmatrix} \varepsilon_{11k} & \varepsilon_{12k} & \cdots & \varepsilon_{1pk} \\ \varepsilon_{21k} & \varepsilon_{22k} & \cdots & \varepsilon_{1pk} \\ \vdots & \vdots & \ddots & \vdots \\ \varepsilon_{n1k} & \varepsilon_{n2k} & \cdots & \varepsilon_{npk} \end{bmatrix}, \tag{2}$$

where $\mathbf{Y}_k$ is an $n \times p$ matrix of response variables for the kth sample, $\mathbf{X}$ is an $n \times (q+1)$ matrix of explanatory variables, $\mathbf{B}$ is a $(q+1) \times p$ matrix of regression parameters, and $\mathbf{E}_k$ is an $n \times p$ matrix of error terms. Note that the vector of error terms follows a p-variate normal distribution with mean vector $\mathbf{0}$ and $p \times p$ covariance matrix as [21]:

$$\mathbf{\Sigma} = \begin{pmatrix} \sigma_{11} & \sigma_{12} & \dots & \sigma_{1p} \\ \sigma_{21} & \sigma_{22} & \dots & \sigma_{2p} \\ \vdots & \vdots & \ddots & \vdots \\ \sigma_{p1} & \sigma_{p2} & \dots & \sigma_{pp} \end{pmatrix}, \tag{3}$$

where σ_{hj} denotes the covariance between error vector terms of the hth and jth response variables at each observation. For the kth random sample, the Ordinary Least Square (OLS) estimator of matrix $\mathbf{B}$ is given by:

$$\hat{\mathbf{B}}_k = (\mathbf{X}_k^{\mathbf{T}} \mathbf{X}_k)^{-\mathbf{1}} \mathbf{X}_k^{\mathbf{T}} \mathbf{Y}_k. \tag{4}$$

3. Existing work: ELRT control charts for simultaneous monitoring of mean vector and covariance matrix in Phase II

In this section, we give a brief review of the proposed ELRT control chart by Eyvazian et al. [21]. The likelihood ratio statistic is given as:

$$\text{ELRT}_k = n \log |\mathbf{\Sigma}| - n \log |E\mathbf{S}_k| + EC_k - np, \qquad k = 1, 2, \dots, \tag{5}$$

in which $\mathbf{\Sigma}$ is covariance matrix of error terms, EC_k and $E\mathbf{S}_k$ are corresponding exponentially weighted moving average statistics given by:

$$EC_k = \alpha C_k + (1-\alpha)\, EC_{k-1}, \tag{6}$$

$$E\mathbf{S}_k = \alpha \mathbf{S}_k + (1-\alpha)\, E\mathbf{S}_{k-1}, \tag{7}$$

where C_k is equal to $\sum_{i=1}^{n} (\mathbf{y}_{ik} - \mathbf{x}_i\mathbf{B})\Sigma^{-1}(\mathbf{y}_{ik} - \mathbf{x}_i\mathbf{B})^T$, in which $(\mathbf{y}_{ik} - \mathbf{x}_i\mathbf{B})$ is the ith row of matrix $(\mathbf{Y}_k - \mathbf{XB})$. $\mathbf{S}_k$ in Eq. (7) is computed as:

$$\mathbf{S}_k = \frac{(\mathbf{Y}_k - \mathbf{X}(E\hat{\mathbf{B}}_k))^T(\mathbf{Y}_k - \mathbf{X}(E\hat{\mathbf{B}}_k))}{n}, \tag{8}$$

where $E\hat{\mathbf{B}}_k$ is exponentially weighted moving average statistic of $\hat{\mathbf{B}}_k$ given by:

$$E\hat{\mathbf{B}}_k = \alpha \hat{\mathbf{B}}_k + (1-\alpha)\, E\hat{\mathbf{B}}_{k-1}. \tag{9}$$

$\hat{\mathbf{B}}_K$ in Eq. (9) is the MLE of $\mathbf{B}$ for the kth sample, which is same as the OLS estimator given in Eq. (4).

4. Proposed control charts

In this section, we propose two control charts including Max-MEWMA and Max-MCUSUM to monitor mean vector and covariance matrix simultaneously in multivariate multiple linear regression profiles.

4.1. Max-MEWMA control chart

Matrix $\hat{\mathbf{B}}_K$ is rewritten as a $1 \times ((q+1)p)$ multivariate normal random vector denoted by $\hat{\boldsymbol{\beta}}_k$:

$$\hat{\boldsymbol{\beta}}_k = (\hat{\beta}_{01k}, \hat{\beta}_{11k}, ..., \hat{\beta}_{q1k}, \hat{\beta}_{02k}, \hat{\beta}_{12k}, ..., \hat{\beta}_{q2k}, ..., \hat{\beta}_{0pk}, \hat{\beta}_{1pk}, ..., \hat{\beta}_{qpk}), \tag{10}$$

when the process is in-control, the expected value and covariance matrix for $\hat{\boldsymbol{\beta}}_k$ are given as follows [21]:

$$E(\hat{\boldsymbol{\beta}}_k) = (\beta_{01}, \beta_{11}, ..., \beta_{q1}, \beta_{02}, \beta_{12}, ..., \beta_{q2}, ..., \beta_{0p}, \beta_{1p}, ..., \beta_{qp}), \tag{11}$$

$$\mathbf{\Sigma}_{\hat{\boldsymbol{\beta}}_k} = \begin{pmatrix} \mathbf{\Sigma}_{11} & \mathbf{\Sigma}_{12} & ... & \mathbf{\Sigma}_{1p} \\ \mathbf{\Sigma}_{21} & \mathbf{\Sigma}_{22} & ... & \mathbf{\Sigma}_{2p} \\ \vdots & \vdots & \ddots & \vdots \\ \mathbf{\Sigma}_{p1} & \mathbf{\Sigma}_{p2} & \dots & \mathbf{\Sigma}_{pp} \end{pmatrix}, \tag{12}$$

where $(\beta_{01}, \beta_{11}, \dots, \beta_{q1}, \beta_{02}, \beta_{12}, \dots, \beta_{q2}, \dots, \beta_{0p}, \beta_{1p}, \dots, \beta_{qp})$ is denoted by $\boldsymbol{\beta}$. Eyvazian et al. [21] have shown that $\mathbf{\Sigma}_{hj}$ is a $(q+1) \times (q+1)$ matrix equal to $[\mathbf{X}^T\mathbf{X}]^{-1}\boldsymbol{\sigma}_{hj}$ where $\boldsymbol{\sigma}_{hj}$ denotes the hjth element of the covariance matrix $\mathbf{\Sigma}$ in Eq. (3).

In this method, we extend the proposed method by Chen et al. [30] for simultaneous monitoring of mean vector and covariance matrix of the regression parameters estimators in the multivariate multiple linear regression profiles. Define:

$$\mathbf{z}_k = \alpha(\hat{\boldsymbol{\beta}}_k - \boldsymbol{\beta}) + (1-\alpha)\,\mathbf{z}_{k-1}, \qquad k = 1, 2, ..., \tag{13}$$

where $\mathbf{z}_0$ is the starting point and it is equal to zero vector. α is the smoothing parameter satisfying $0 \leq \alpha \leq 1$. We have:

$$\boldsymbol{\Sigma}_{\mathbf{z}_k} = \frac{\alpha}{2-\alpha}\left[1-(1-\alpha)^{2k}\right]\boldsymbol{\Sigma}_{\hat{\boldsymbol{\beta}}_k}, \tag{14}$$

$$T_k = \frac{(2-\alpha)}{\alpha\left[1-(1-\alpha)^{2k}\right]}\,\mathbf{z}_k^T\,\boldsymbol{\Sigma}_{\hat{\boldsymbol{\beta}}}^{-1}\,\mathbf{z}_k \sim \chi^2_{(q+1)p,\delta^2}. \tag{15}$$

In Eq. (15), $(q+1)p$ and δ^2 are respectively the degrees of freedom and the non-centrality parameter of the non-central chi-square distribution with:

$$\delta^2 = \left((2-\alpha)/\alpha\left[1-(1-\alpha)^{2k}\right]\right)(\boldsymbol{\beta}_b - \boldsymbol{\beta}_g)'$$
$$\boldsymbol{\Sigma}^{-1}(\boldsymbol{\beta}_b - \boldsymbol{\beta}_g) \sim \chi^2_{(q+1)p,\delta^2}, \tag{16}$$

where $\boldsymbol{\beta}_g$ is good mean (when the process is in-control) and $\boldsymbol{\beta}_b$ is bad mean (when the process is out-of-control). We define the statistic for monitoring the process mean vector as:

$$C_k = \Phi^{-1}\left[H_{(q+1)p}\left\{\frac{(2-\alpha)}{\alpha\left[1-(1-\alpha)^{2k}\right]}\mathbf{z}_k^T\Sigma_{\hat{\boldsymbol{\beta}}}^{-1}\mathbf{z}_k\right\}\right], \tag{17}$$

where $H_{(q+1)p}(.)$ is the chi-square distribution function with $(q+1)p$ degrees of freedom, $\Phi(.)$ is the standard normal cumulative distribution function, and Φ^{-1} is the inverse of $\Phi(.)$.

For monitoring process variability, we define:

$$W_k = \sum_{i=1}^{n}(\mathbf{y}_{ik} - \mathbf{x}_i\mathbf{B})\Sigma^{-1}(\mathbf{y}_{ik} - \mathbf{x}_i\mathbf{B})^T, \tag{18}$$

such that W_k is the chi-square distribution with np degrees of freedom.

$$g_k = (1-\alpha)g_{k-1} + \alpha\Phi^{-1}\left\{H_{np}(W_k)\right\}, \tag{19}$$

where g_0 is the starting point and it is equal to zero.α is the smoothing parameter, $0 \leq \alpha \leq 1$. We have $E(g_k) = 0$ and $Var(g_k) = \frac{\alpha}{2-\alpha}[1-(1-\alpha)^{2k}]$.

The statistic for monitoring the process variability is defined as:

$$S_k = \sqrt{\frac{2-\alpha}{\alpha(1-(1-\alpha)^{2k})}}\,g_k. \tag{20}$$

Combining C_k and S_k defines a statistic for a single control chart as:

$$M_k = \max\left\{|C_k|, |S_k|\right\} \qquad k = 1, 2, ... \tag{21}$$

Since M_k is the maximum $|C_k|$ and $|S_k|$, which are based on two Multivariate Exponentially Weighted Moving Average (MEWMA) statistics, it is natural to name the control chart, based on M_k, Max–MEWMA control chart Chen et al.[30]. A large value of M_k means that the process mean vector and/or covariance matrix has shifted away from $\boldsymbol{\beta}$ and $\boldsymbol{\Sigma}$, respectively. Because M_k is non-negative, the initial state of the Max–MEWMA control chart is based only on an upper control limit (h). If $M_k > h$, the control chart triggers an out-of-control alarm, where $h > 0$ is chosen to achieve a specified in-control ARL.

4.2. Max-MCUSUM control chart

In this section we explain the structure of Max–MCUSUM control chart to use it for monitoring multivariate multiple linear regression profiles in Phase II. The cumulative sum (CUSUM) procedure for monitoring mean vector of multivariate quality characteristics signals when the value of S_k becomes greater than L.

$$S_k = \max\left(0, S_{k-1} + \log\frac{f_b(x_k)}{f_g(x_k)}\right) > L, \tag{22}$$

where f_g and f_b are probability density functions corresponding to quality characteristics under in-control and out-of-control conditions, respectively, and L is a constant that determines the Upper Control Limit (UCL) of the statistic in Eq. (22). In this section, we extend the method proposed by Cheng and Thaga [31].

We assume that $\boldsymbol{\beta}_k$ comes from a multivariate normal distribution with either a good mean, $\boldsymbol{\beta}_g$, for in-control process or bad mean, $\boldsymbol{\beta}_b$ ($\boldsymbol{\beta}_b$=$\boldsymbol{\beta}_g + \boldsymbol{\delta}$), for out-of-control process. Note that the covariance matrix of error terms, $\boldsymbol{\Sigma}$, is assumed known. For a multivariate normal distribution, the CUSUM chart is developed through the likelihood ratio given as:

$$\frac{f_b(x_k)}{f_g(x_k)} =$$
$$\frac{(2\pi)^{-p/2}\left|\Sigma_{\hat{\boldsymbol{\beta}}_k}^{-1}\right|^{-1/2}\exp(-0.5(\hat{\boldsymbol{\beta}}_k - \boldsymbol{\beta}_b)\Sigma_{\hat{\boldsymbol{\beta}}_k}^{-1}(\hat{\boldsymbol{\beta}}_k - \boldsymbol{\beta}_b)')}{(2\pi)^{-p/2}\left|\Sigma_{\hat{\boldsymbol{\beta}}_k}^{-1}\right|^{-1/2}\exp(-0.5(\hat{\boldsymbol{\beta}}_k - \boldsymbol{\beta}_g)\Sigma_{\hat{\boldsymbol{\beta}}_k}^{-1}(\hat{\boldsymbol{\beta}}_k - \boldsymbol{\beta}_g)')}. \tag{23}$$

Taking natural logarithms (see Appendix A), we obtain:

$$\log\frac{f_b(x_k)}{f_g(x_k)} = (\boldsymbol{\beta}_b - \boldsymbol{\beta}_g)\boldsymbol{\Sigma}_{\hat{\boldsymbol{\beta}}_k}^{-1}\hat{\boldsymbol{\beta}}'_k - 0.5(\boldsymbol{\beta}_b + \boldsymbol{\beta}_g)$$
$$\boldsymbol{\Sigma}_{\hat{\boldsymbol{\beta}}_k}^{-1}(\boldsymbol{\beta}_b - \boldsymbol{\beta}_g)'. \tag{24}$$

Replacing Eq. (24) into Eq. (22), CUSUM statistic for the multivariate normal process is obtained. Note that both sides of Eq. (24) are divided by a constant value. CUSUM statistic for monitoring the multivariate multiple linear regression profile is given as follows:

$$S_k = \max(S_{k-1} + a\hat{\boldsymbol{\beta}}_k - w, 0), \tag{25}$$

where:

$$a = \frac{(\boldsymbol{\beta}_b - \boldsymbol{\beta}_g)\boldsymbol{\Sigma}^{-1}_{\hat{\boldsymbol{\beta}}_k}}{\sqrt{(\boldsymbol{\beta}_b - \boldsymbol{\beta}_g)\boldsymbol{\Sigma}^{-1}_{\hat{\boldsymbol{\beta}}_k}(\boldsymbol{\beta}_b - \boldsymbol{\beta}_g)'}}, \tag{26}$$

and:

$$w = 0.5\frac{(\boldsymbol{\beta}_b - \boldsymbol{\beta}_g)\boldsymbol{\Sigma}^{-1}_{\hat{\boldsymbol{\beta}}_k}(\boldsymbol{\beta}_b - \boldsymbol{\beta}_g)'}{\sqrt{(\boldsymbol{\beta}_b - \boldsymbol{\beta}_g)\boldsymbol{\Sigma}^{-1}_{\hat{\boldsymbol{\beta}}_k}(\boldsymbol{\beta}_b - \boldsymbol{\beta}_g)'}}. \tag{27}$$

Define the non-centrality parameter as:

$$D = \sqrt{(\boldsymbol{\beta}_b - \boldsymbol{\beta}_g)\boldsymbol{\Sigma}^{-1}_{\hat{\boldsymbol{\beta}}_k}(\boldsymbol{\beta}_b - \boldsymbol{\beta}_g)'}, \tag{28}$$

and:

$$Z_k = a(\hat{\boldsymbol{\beta}}_k - \boldsymbol{\beta}_g)'. \tag{29}$$

The CUSUM control chart for detecting a shift in the multivariate multiple profiles regression coefficients vector is written as:

$$U_k = \max\,(0,\, U_{k-1} + Z_k - 0.5D). \tag{30}$$

By using the likelihood ratio test technique above and assuming the good state and bad state, Healy [39] developed a CUSUM chart for the process standard deviation. When the process is in a good state, $\hat{\boldsymbol{\beta}}$ is distributed as multivariate normal with good mean, $\boldsymbol{\beta}_g$ and covariance matrix, $\boldsymbol{\Sigma}_{\hat{\boldsymbol{\beta}}}$. In the case of shift in variability, we assume that the covariance matrix shifts to $b\boldsymbol{\Sigma}_{\hat{\boldsymbol{\beta}}}$ for $b > 0$ and mean vector does not change.

The likelihood ratio for process standard deviation is given in Eq. (31) as shown in Box I. Taking natural logarithms (see Appendix B), we obtain:

$$\log\frac{f_b(x_k)}{f_g(x_k)} = \frac{-1}{2}\log b + 0.5(\hat{\boldsymbol{\beta}}_k - \boldsymbol{\beta}_g)$$
$$\boldsymbol{\Sigma}^{-1}_{\hat{\boldsymbol{\beta}}_k}(\hat{\boldsymbol{\beta}}_k - \boldsymbol{\beta}_g)'(1 - \frac{1}{b}). \tag{32}$$

The CUSUM control chart for detecting a shift in the covariance matrix of a multivariate multiple regression profile is written as:

$$S_k = \max\,(S_{k-1} + (\hat{\boldsymbol{\beta}}_k - \boldsymbol{\beta}_g)\boldsymbol{\Sigma}^{-1}_{\hat{\boldsymbol{\beta}}_k}(\hat{\boldsymbol{\beta}}_k - \boldsymbol{\beta}_g)' - \nu, 0), \tag{33}$$

$$\nu = \log(b)\left(\frac{b}{b-1}\right). \tag{34}$$

To design a single multivariate CUSUM control chart for simultaneous monitoring of mean vector and covariance matrix in the multivariate multiple linear regression profiles in Phase II, we use the following transformation:

$$Y_k = \Phi^{-1}\Big[H_{(q+1)p}\Big\{(\hat{\boldsymbol{\beta}}_k - \boldsymbol{\beta}_g)\boldsymbol{\Sigma}^{-1}_{\hat{\boldsymbol{\beta}}_k}(\hat{\boldsymbol{\beta}}_k - \boldsymbol{\beta}_g)'\Big\}\Big], \tag{35}$$

where $H_{(q+1)p}(\cdot)$ is the chi-square distribution function with $(q+1)p$ degrees of freedom, $\Phi(\cdot)$ is the standard normal cumulative distribution function, and Φ^{-1} is the inverse of $\Phi(\cdot)$.

For monitoring the process variability, we define:

$$V_k = \max\,(0, Y_k - \nu + V_{k-1}). \tag{36}$$

Combining U_k and V_k defines a statistic for multivariate single control chart as:

$$M_k = \max\,(U_k, V_k). \tag{37}$$

The proposed control chart is called Maximum Multivariate CUSUM (Max-MCUSUM) control chart, because the maximum CUSUM statistic is applied. Since M_k is non-negative, the initial state of the Max-MCUSUM control chart is based only on an upper control limit (L). If $M_k > L$, the control chart triggers an out-of-control alarm, where $L > 0$ is chosen to achieve a specified in-control ARL.

5. Diagnosing procedure

In a diagnosing procedure for Max-MEWMA control chart, the following algorithm is proposed to determine the source and the direction of the shift:

- **Case 1**: $M_k = |C_k| > UCL$ and $|S_k| \leq UCL$. It indicates that only the process mean experiences a shift. If $C_k > 0$, the shift is increasing and it is decreasing if $C_k < 0$,

$$\frac{f_b(x_k)}{f_g(x_k)} = \frac{(2\pi)^{-p/2}\left|b\boldsymbol{\Sigma}_{\hat{\boldsymbol{\beta}}_k}\right|^{-1/2}\exp(-0.5(\hat{\boldsymbol{\beta}}_k - \boldsymbol{\beta}_g)(b\boldsymbol{\Sigma}_{\hat{\boldsymbol{\beta}}_k})^{-1}(\hat{\boldsymbol{\beta}}_k - \boldsymbol{\beta}_b)')}{(2\pi)^{-p/2}\left|\boldsymbol{\Sigma}_{\hat{\boldsymbol{\beta}}_k}\right|^{-1/2}\exp(-0.5(\hat{\boldsymbol{\beta}}_k - \boldsymbol{\beta}_g)\boldsymbol{\Sigma}^{-1}_{\hat{\boldsymbol{\beta}}_k}(\hat{\boldsymbol{\beta}}_k - \boldsymbol{\beta}_g)')}. \tag{31}$$

Box I

- **Case 2**: $|C_k| \leq UCL$ and $M_k = |S_k| > UCL$. It shows that only the process variability experiences a shift. If $S_k > 0$, the shift is increasing and it is a decreasing one if $S_k < 0$,
- **Case 3**: Both $|C_k|$ and $|S_k|$ are larger than UCL. Simultaneous change occurs in the process mean and variance. The change direction in mean and variance of the process is determined by the methods explained in Cases 1 and 2.

The same procedure is used for Max-MCUSUM control chart to diagnose whether the mean vector or covariance matrix is responsible for out-of-control signal and direction of the shift.

6. Performance evaluation

In this section, we present a numerical example based on simulation study in order to investigate the performance of the proposed control charts in detecting different out-of-control scenarios. Different approaches can be used for calculating the ARL, e.g. Monte Carlo simulations, Integral equations, and Markov chains approximations. In this paper, Monte Carlo simulation is used in order to calculate the ARL and SDRL in both proposed control charts and the existing ELRT control chart. The results of simulation study in terms of two criteria, including the ARL and SDRL, are obtained by 10000 replicates. Without loss of generality, in the entire MEWMA statistic, the value of smoothing parameter, α, is set equal to 0.2 as generally used in the literature. The underlying multivariate multiple linear regression profile model considered in this paper is:

$$y_1 = 3 + 2x_1 + x_2 + \varepsilon_1,$$

$$y_2 = 2 + x_1 + x_2 + \varepsilon_2.$$

The pairs of observations (2,1), (4,2), (6,3), and (8,2) are considered as the values for explanatory variables x_1 and x_2. The vector of error terms $(\varepsilon_1, \varepsilon_2)$ follows a bivariate normal random variable with mean vector zero and known covariance matrix:

$$\mathbf{\Sigma} = \begin{pmatrix} \sigma_1^2 & \rho\sigma_1\sigma_2 \\ \rho\sigma_1\sigma_2 & \sigma_2^2 \end{pmatrix},$$

where $\sigma_1^2 = 1$ and $\sigma_2^2 = 1$ based on [21]. To investigate the effect of correlation between profiles, different values of ρ, namely, $\rho = 0.1$ and $\rho = 0.5$, are used in our simulation studies for individual shifts. For simultaneous shifts, the correlation between response variables is set equal to 0.5.

For ELRT control chart, the upper control limit is set equal to 3.79 to give an in-control ARL of approximately 200. In the Max-MEWMA control chart, the upper control limit is set equal to 2.94 and the upper control limit for Max-MCUSUM control chart equals 3.88, which gives an in-control ARL of 200. In the Max-MCUSUM control chart, the magnitude of the shift in process variability (b) is equal to 1.2 and $\boldsymbol{\beta}_b$ is considered equal to the smallest intercept and slope parameters after shift, i.e.:

$$\boldsymbol{\beta}_b = (3.2, 2.025, 1.025, 2.2, 1.025, 1.025).$$

Several different types of the intercept, slope, and standard deviation shifts are considered in the simulation study. The ARL and SDRL values for different shifts in the β_{01} in units of σ_1 are summarized in Table 1. The results show that the Max-CUSUM control chart scheme performs better than the other methods under $\rho = 0.1$. Moreover, Max-MEWMA control chart is better than other control charts under $\rho = 0.5$ when shifts in the intercept are large. Similar results are obtained for sustained shifts in the intercept of the second profile.

The ARL and SDRL values for different shifts in β_{11} in units of σ_1 are also given in Table 2. Similar to the results of Table 1, for $\rho = 0.1$, the Max-CUSUM control chart scheme performs better than the other methods and the Max-MEWMA control chart is superior to the ELRT control chart under large shifts in the slope. For $\rho = 0.5$, except in $\lambda_1 = 0.025$ and 0.05, the performance of Max-MEWMA control chart is better than that of Max-MCUSUM and ELRT control charts. According to the ARL and SDRL results, the performance of the ELRT and Max-MEWMA control chart schemes improves as the value of ρ increases and the performance of Max-MCUSUM control chart for large shifts in β_{11} decreases. Also, similar results are obtained for the sustained shifts in β_{12}, i.e., the slope of the second profile.

Table 3 shows the out-of-control simulated ARL and SDRL values for shifts in variance of the error term in the first profile from σ_1 to $\gamma\sigma_1$. The results show that the performance of Max-MEWMA control chart is uniformly better than that of ELRT and Max-MCUSUM control charts and the performance of ELRT control chart is superior to that of Max-MCUSUM control chart. Increasing the value of ρ leads to better performance in all of the control charts. The results for shift in σ_2 are similar to those for shift in σ_1. Hence, the results are not reported in this paper.

Tables 4 to 6 show the simultaneous shifts in the intercept of profiles, shifts in the slope of profiles, and shifts in the standard deviations of profiles, respectively. As shown in Tables 4 and 5, for simultaneous shifts in the regression coefficients of profiles, Max-MCUSUM control chart outperforms the other control charts. In addition, when the magnitude of shifts in the intercept and slope increases, the performance of Max-MEWMA relative to ELRT control chart in terms

Table 1. The simulated out-of-control ARL and SDRL values under the intercept shifts from β_{01} to $\beta_{01}+\lambda_0\sigma_1$ (in-control ARL = 200).

$\rho = 0.1$		λ_0									
		0.2	**0.4**	**0.6**	**0.8**	**1**	**1.2**	**1.4**	**1.6**	**1.8**	**2**
ELRT	ARL	90.32	28.61	13.65	8.64	6.23	4.81	3.87	3.22	2.75	2.45
	SDRL	79.66	19.79	6.83	3.43	2.15	1.49	1.17	0.95	0.81	0.68
Max-MEWMA	ARL	133.5	36.41	14.19	8.06	5.66	4.40	3.65	3.10	2.73	2.39
	SDRL	134.1	30.42	8.78	3.80	2.04	1.33	1.01	0.79	0.67	0.58
Max-MCUSAM	ARL	71.39	23.78	11.92	7.46	5.48	4.29	3.52	2.97	2.59	2.30
	SDRL	65.89	19.00	7.85	4.00	2.55	1.78	1.30	1.00	0.79	0.65
$\rho = 0.5$		λ_0									
		0.2	**0.4**	**0.6**	**0.8**	**1**	**1.2**	**1.4**	**1.6**	**1.8**	**2**
ELRT	ARL	75.91	21.93	10.91	6.99	5.12	3.98	3.20	2.74	2.27	1.96
	SDRL	64.46	14.42	4.84	2.47	1.64	1.21	0.93	0.76	0.64	0.55
Max-MEWMA	ARL	112.8	25.79	10.51	6.46	4.66	3.71	3.08	2.67	2.24	1.94
	SDRL	111.2	20.22	5.69	2.59	1.49	1.01	0.77	0.65	0.57	0.48
Max-MCUSAM	ARL	58.80	24.50	12.85	8.40	5.99	4.52	3.57	2.89	2.45	2.13
	SDRL	54.39	20.05	8.65	4.81	2.91	1.97	1.33	0.97	0.74	0.60

Table 2. The simulated out-of-control ARL and SDRL values under the intercept shifts from β_{11} to $\beta_{11}+\lambda_1\sigma_1$ (in-control ARL = 200).

$\rho = 0.1$		λ_1									
		0.025	**0.05**	**0.075**	**0.1**	**0.125**	**0.15**	**0.175**	**0.2**	**0.225**	**0.25**
ELRT	ARL	131.34	57.29	27.17	15.95	11.00	8.25	6.62	5.46	4.64	4.01
	SDRL	124.46	47.44	19.06	8.49	4.97	3.15	2.34	1.78	1.43	1.21
Max-MEWMA	ARL	168.8	84.15	33.80	17.01	10.58	7.74	6.07	5.00	4.27	3.75
	SDRL	169.7	80.72	28.42	11.20	5.7	3.46	2.33	1.68	1.28	1.04
Max-MCUSAM	ARL	108.41	46.12	23.42	14.23	9.81	7.33	5.88	4.94	4.22	3.67
	SDRL	100.65	40.05	18.84	10.08	5.98	3.97	2.84	2.19	1.71	1.37
$\rho = 0.5$		λ_1									
		0.025	**0.05**	**0.075**	**0.1**	**0.125**	**0.15**	**0.175**	**0.2**	**0.225**	**0.25**
ELRT	ARL	115.23	45.04	21.43	12.67	8.85	6.77	5.45	4.50	3.84	3.29
	SDRL	105.10	35.76	13.60	6.10	3.51	2.41	1.78	1.38	1.15	0.96
Max-MEWMA	ARL	161.31	62.82	20.20	12.56	8.24	6.14	4.98	4.15	3.59	3.17
	SDRL	160.62	58.04	18.64	7.51	3.84	2.35	1.66	1.22	0.98	0.81
Max-MCUSAM	ARL	86.44	41.29	23.61	15.38	10.90	8.28	6.50	5.26	4.36	3.71
	SDRL	81.93	36.17	19.12	11.27	7.03	4.68	3.33	2.41	1.84	1.42

Table 3. The simulated out-of-control ARL and SDRL values under the shifts from σ_1 to $\gamma\sigma_1$ (in-control ARL = 200).

$\rho = 0.1$		γ									
		1.2	**1.4**	**1.6**	**1.8**	**2**	**2.2**	**2.4**	**2.6**	**2.8**	**3**
ELRT	ARL	43.62	13.97	7.69	5.14	3.92	3.14	2.67	2.31	2.04	1.83
	SDRL	36.24	9.17	4.32	2.73	1.98	1.59	1.34	1.13	1.00	0.87
Max-MEWMA	ARL	41.58	13.18	6.93	4.80	3.69	3.07	2.60	2.28	2.06	1.88
	SDRL	37.29	9.55	4.23	2.55	1.85	1.46	1.18	1.02	0.91	0.83
Max-MCUSAM	ARL	136.8	45.67	17.15	9.15	6.02	4.61	3.61	3.05	2.68	2.39
	SDRL	130.7	41.12	14.98	7.34	4.28	2.63	1.89	1.53	1.19	1.05
$\rho = 0.5$		γ									
		1.2	**1.4**	**1.6**	**1.8**	**2**	**2.2**	**2.4**	**2.6**	**2.8**	**3**
ELRT	ARL	39.56	12.65	6.79	4.68	3.53	2.82	2.43	2.14	1.89	1.69
	SDRL	31.80	7.96	3.72	2.42	1.76	1.39	1.20	1.03	0.92	0.79
Max-MEWMA	ARL	39.23	12.18	6.48	4.45	3.41	2.77	2.39	2.12	1.91	1.73
	SDRL	36.12	8.84	3.92	2.39	1.65	1.31	1.09	0.95	0.86	0.77
Max-MCUSAM	ARL	99.42	36.26	14.78	7.98	5.38	4.04	3.27	2.78	2.41	2.18
	SDRL	96.04	33.16	11.88	5.67	3.51	2.40	1.87	1.54	1.28	1.14

Table 4. The simulated out-of-control ARL and SDRL values under simultaneous shifts from β_{01} to $\beta_{01} + \lambda_0\sigma_1$ in the first profile and β_{02} to $\beta_{02} + \delta_0\sigma_2$ in the second profile with $\rho = 0.5$ (in-control ARL = 200).

		λ_0									
		0.2		**0.4**		**0.6**		**0.8**		**1**	
δ_0	**Control chart**	**ARL**	**SDRL**	**ARL**	**SDRL**	**ARL**	**SDRL**	**ARL**	**SDRL**	**ARL**	**SDRL**
	ELRT	75.55	66.70	28.96	19.89	13.27	6.62	8.20	3.12	5.80	1.91
0.2	Max-MEWMA	111.0	106.8	37.08	30.74	13.55	8.24	7.62	3.36	5.25	1.81
	Max-MCUSAM	24.38	19.91	13.00	8.86	8.50	4.93	6.21	3.08	4.52	2.11
	ELRT	29.35	20.51	22.46	14.49	13.31	6.74	8.65	3.47	6.19	2.07
0.4	Max-MEWMA	37.10	31.63	25.92	20.04	13.55	8.11	8.20	3.82	5.64	2.04
	Max-MCUSAM	13.19	9.03	8.53	4.96	6.23	3.10	5.01	2.26	4.10	1.63
	ELRT	13.44	6.78	13.32	6.61	10.95	4.83	8.19	3.13	6.20	2.07
0.6	Max-MEWMA	13.54	8.22	13.62	8.44	10.62	5.79	7.54	3.28	5.63	1.99
	Max-MCUSAM	8.58	5.03	6.21	3.03	4.90	2.16	4.12	1.66	3.49	1.27
	ELRT	8.24	3.16	8.68	3.46	8.14	3.16	6.98	2.53	5.78	1.93
0.8	Max-MEWMA	7.61	3.31	8.06	3.67	7.64	3.40	6.44	2.56	5.30	1.83
	Max-MCUSAM	6.19	2.80	4.91	2.15	4.11	1.64	3.53	1.28	3.05	1.04
	ELRT	5.82	1.91	6.19	2.05	6.29	2.18	5.76	1.91	5.10	1.60
1	Max-MEWMA	5.26	1.80	5.66	2.07	5.70	2.09	5.27	1.83	4.67	1.50
	Max-MCUSAM	4.49	2.06	4.09	1.68	3.52	1.29	3.07	1.05	2.75	0.88

Table 5. The simulated out-of-control ARL and SDRL values under simultaneous shifts from β_{11} to $\beta_{11} + \lambda_1\sigma_1$ in the first profile and β_{12} to $\beta_{12} + \delta_1\sigma_2$ in the second profile with $\rho = 0.5$ (in-control ARL = 200).

		λ_1									
		0.025		**0.05**		**0.075**		**0.1**		**0.125**	
δ_1	**Control chart**	**ARL**	**SDRL**	**ARL**	**SDRL**	**ARL**	**SDRL**	**ARL**	**SDRL**	**ARL**	**SDRL**
	ELRT	118.0	107.7	57.80	48.81	26.81	18.47	14.93	8.18	10.09	4.35
0.025	Max-MEWMA	157.1	155.1	84.01	79.32	32.85	26.54	15.72	10.22	9.65	5.03
	Max-MCUSAM	41.87	36.73	23.92	19.53	15.44	11.16	10.93	6.92	8.32	4.81
	ELRT	57.42	48.06	44.77	34.76	26.46	17.98	16.23	8.98	10.90	4.96
0.05	Max-MEWMA	86.09	82.31	63.55	59.56	33.73	28.31	17.35	11.86	10.60	5.77
	Max-MCUSAM	24.03	19.37	15.37	11.35	10.98	7.06	8.32	4.75	6.79	3.42
	ELRT	26.43	17.88	26.74	18.42	21.24	12.83	15.22	8.11	10.88	4.84
0.075	Max-MEWMA	33.16	27.69	33.33	27.32	24.09	18.45	15.82	10.30	10.59	5.58
	Max-MCUSAM	15.55	11.11	10.99	7.20	8.35	4.82	6.76	3.47	5.68	2.67
	ELRT	15.14	8.31	16.23	8.99	15.09	8.11	12.53	6.02	10.07	4.35
0.1	Max-MEWMA	15.70	10.34	17.24	11.54	15.82	10.35	12.58	7.36	9.66	4.83
	Max-MCUSAM	11.02	7.09	8.22	4.62	6.83	3.58	5.66	2.63	4.92	2.15
	ELRT	10.11	4.28	11.12	5.05	10.93	4.92	10.13	4.27	8.83	3.50
0.125	Max-MEWMA	9.76	5.07	10.55	5.69	10.43	5.82	9.58	4.79	8.32	3.86
	Max-MCUSAM	8.37	4.82	6.82	3.57	5.69	2.67	4.87	2.14	4.29	1.76

Table 6. The simulated out-of-control ARL and SDRL values under simultaneous shifts from σ_1 to $\gamma_0\sigma_1$ and σ_2 to $\gamma_1\sigma_2$ with $\rho = 0.5$ (in-control ARL=200).

		γ_0									
		1.1		**1.2**		**1.3**		**1.4**		**1.5**	
γ_1	**Control chart**	**ARL**	**SDRL**	**ARL**	**SDRL**	**ARL**	**SDRL**	**ARL**	**SDRL**	**ARL**	**SDRL**
	ELRT	66.31	60.10	34.11	27.42	18.90	13.38	12.27	7.91	8.80	5.21
1.1	Max-MEWMA	46.19	43.11	23.04	18.93	13.98	10.33	9.63	6.32	7.22	4.38
	Max-MCUSAM	106.2	101.7	72.87	70.24	44.51	40.83	27.45	24.04	17.70	14.55
	ELRT	33.98	27.24	23.63	17.94	15.55	10.70	10.97	6.87	8.18	4.65
1.2	Max-MEWMA	24.04	20.12	14.72	10.80	10.41	7.01	7.74	4.74	6.22	3.57
	Max-MCUSAM	72.11	67.51	48.30	44.42	30.87	26.78	20.33	17.53	13.72	10.96
	ELRT	18.87	13.47	15.48	10.41	12.02	7.60	9.38	5.58	7.33	4.11
1.3	Max-MEWMA	14.02	10.22	10.42	6.84	8.03	4.91	6.47	3.66	5.34	2.80
	Max-MCUSAM	44.64	41.57	31.11	27.15	21.12	17.93	15.00	11.94	10.92	8.11
	ELRT	12.11	7.61	10.81	6.55	9.19	5.38	7.54	4.19	6.42	3.43
1.4	Max-MEWMA	9.75	6.35	7.81	4.74	6.51	3.56	5.44	2.86	4.68	2.30
	Max-MCUSAM	27.72	24.26	20.16	16.92	15.04	11.87	11.47	8.45	8.96	6.34
	ELRT	8.68	5.17	8.16	4.6 9	7.27	4.06	6.38	3.46	5.54	2.91
1.5	Max-MEWMA	7.22	4.33	6.16	3.45	5.36	2.74	4.72	2.38	4.18	2.02
	Max-MCUSAM	17.47	14.33	13.95	10.75	11.00	8.08	9.07	6.44	7.44	4.81

Table 7. The simulated out-of-control ARL and SDRL values under simultaneous shifts from β_{11} to $\beta_{11} + \lambda_1\sigma_1$ and σ_1 to $\gamma_0\sigma_1$ with $\rho = 0.5$ (in-control ARL = 200).

		γ_0									
		0.2		**0.4**		**0.6**		**0.8**		**1.0**	
γ_0	**Control chart**	**ARL**	**SDRL**	**ARL**	**SDRL**	**ARL**	**SDRL**	**ARL**	**SDRL**	**ARL**	**SDRL**
	ELRT	48.17	39.33	14.52	8.91	7.65	3.81	5.08	2.31	3.73	1.61
1.1	Max-MEWMA	58.93	54.63	15.03	10.70	7.49	4.09	4.96	2.37	3.70	1.57
	Max-MCUSAM	49.49	45.43	19.77	15.69	10.56	7.41	6.61	3.99	4.75	2.56
	ELRT	27.05	20.61	8.60	4.72	4.90	2.41	3.37	1.61	2.57	1.20
1.2	Max-MEWMA	29.71	26.03	8.69	5.55	4.78	2.48	3.35	1.56	2.65	1.18
	Max-MCUSAM	41.43	37.72	14.24	11.25	7.11	4.71	4.55	2.62	3.26	1.78
	ELRT	16.60	11.36	5.76	2.98	3.38	1.65	2.42	1.18	1.93	0.92
1.3	Max-MEWMA	16.88	13.08	5.56	3.09	3.34	1.60	2.45	1.12	1.99	0.88
	Max-MCUSAM	32.13	28.50	9.29	6.50	4.77	2.94	3.17	1.73	2.42	1.25
	ELRT	11.28	6.91	4.21	2.10	2.59	1.27	1.91	0.92	1.58	0.72
1.4	Max-MEWMA	11.05	7.66	4.06	2.07	2.58	1.17	1.97	0.86	1.61	0.70
	Max-MCUSAM	23.80	20.42	6.41	4.15	3.45	1.96	2.45	1.29	1.95	0.99
	ELRT	8.30	4.72	3.31	1.65	2.11	1.03	1.62	0.73	1.37	0.58
1.5	Max-MEWMA	7.94	4.93	3.24	1.54	2.14	0.94	1.68	0.73	1.41	0.59
	Max-MCUSAM	17.08	14.02	4.77	2.97	2.75	1.49	2.00	1.05	1.65	0.81

of ARL and SDRL improves. According to Table 6, the Max-MEWMA control chart performs better than the two other control charts in detecting simultaneous shifts in both standard deviations.

Table 7 shows the out-of-control ARL and SDRL under simultaneous shifts in the intercept and standard deviation of the first profile. The results show that under small shifts in the standard deviation, ELRT control chart has better performance than the other control charts. When the magnitude of shifts in standard deviation increases, the performance of Max-MEWMA control chart improves relative to the other control charts.

6.1. Evaluating diagnosing procedure

For all scenarios of the shifts in Tables 8 and 9, the diagnosing procedures of the schemes are also implemented. In Tables 8 and 9, there are three rows named U, V, and UV for each control chart that represent the mean shifts, variance shifts, and simultaneous shifts, respectively. Table 8 shows the performance of diagnosing procedures (in percent) under individual shifts in the regression parameters when the value of ρ is equal to 0.5 and signal is triggered by both the proposed control charts. The results show that the diagnosing procedure in Max-MEWMA control chart under small and medium shifts in the intercept, slope, and standard deviation performs excellently while this procedure does not perform well in diagnosing large shifts in the intercept, slope, and standard deviation. Also, Table 8 shows that Max-MCUSUM control chart performs well in diagnosing under medium and large shifts in standard deviation while Max-MCUSUM control chart performs satisfactorily in diagnosing small and medium shifts in the intercept and slope. Table 9 shows the performance of the diagnosing procedure in Max-MEWMA and Max-MCUSUM under simultaneous shifts in the regression parameters. The results show that the diagnosing procedure in Max-MEWMA control chart performs well in simultaneous small and medium shifts in β_{01} and β_{02} as well as β_{11} and β_{12}. However, Max-MEWMA diagnosing procedure does not perform satisfactorily under simultaneous large shifts in standard deviation. Finally, the diagnosing procedure under all simultaneous shifts in the Max-MCUSUM control chart shows excellent performance.

7. A real case study

In this section, we illustrate how the proposed control chart can be applied to the calibration case at the

Table 8. The results (accuracy percent) of individual shifts in the intercept, slope, and the standard deviation of the first profiles ($\rho = 0.5$).

Proposed control chart											
		Intercept shifts from β_{01} to $\beta_{01} + \lambda_0\sigma_1$ in the first profile									
Proposed control chart	λ_0	**0.2**	**0.4**	**0.6**	**0.8**	**1**	**1.2**	**1.4**	**1.6**	**1.8**	**2**
Max-MEWMA	U	75.24%	91.34%	92.55%	87.95%	77.49%	61.81%	43.71 %	37.31%	23.85%	16.96%
	V	22.49%	5.40%	2.80%	2.64%	3.35%	4.30%	5.27%	6.58%	7.52%	9.73%
	UV	2.27%	3.26%	4.65%	9.41%	19.16%	33.89%	51.01%	56.11%	68.63%	73.31%
Max-MCUSAM	U	99.61%	99.38%	97.94%	93.46%	81.51%	54.24%	43.43%	33.46%	24. 00%	17.12%
	V	0.32%	0.46%	1.49%	3.95%	10.29%	19.11%	29.24%	30.80 %	33.23%	37.75%
	UV	0.06%	0.16%	0.57%	2.59%	8.20%	16.65%	27.34%	35.74 %	42.76%	45.12%
		Standard deviation shifts from σ to $\gamma\sigma_1$									
Proposed control chart	γ	1.1	1.2	1.3	1.4	1.5	1.6	1.7	1.8	1.9	2
Max-MEWMA	U	38.00%	13.29%	5.19%	1.86%	0.59%	0.19%	0.08%	0.06%	0%	0%
	V	58.90%	80.54%	84.64%	82.13%	74.66%	61.88%	47.78%	34.16%	24.31%	16.74%
	UV	3.10%	6.17%	10.17%	16.01%	24.75%	37.94%	52.15%	65.77%	75.69%	83.26%
Max-MCUSAM	U	96.16%	64.11%	17.15%	4.54%	1.65%	0.6%	0.25%	0.05%	0.05%	0%
	V	3.66%	34.23%	78.43%	89.85%	91.85%	91.74%	90.39%	88.31%	85.52%	81.41%
	UV	0.18%	1.66%	4.42%	5.61%	6.50%	7.66%	9.36%	11.64%	14.42%	18.59%
		Slope shifts from β_{11} to $\beta_{11} + \lambda_1\sigma_1$ in the first profile									
Proposed control chart	λ_1	0.025	0.05	0.075	0.1	0.125	0.15	0.175	0 .2	0.225	0.25
Max-MEWMA	U	65.49%	84.62%	91.76%	92.49%	90.86%	87.14%	80.40%	71.64%	59.34%	47.14%
	V	32.57%	12.71%	4.94%	3.31%	2.88%	2.21%	2.66%	3.20%	3.91%	4.89%
	UV	1.94%	2.66%	3.30%	4.20%	6.26%	10.65%	16.94%	25.16 %	36.75%	47.98%
Max-MCUSAM	U	99.55%	99.55%	99.45%	98.36%	96.49%	92.03%	84.79%	72 .69%	59.90%	45.06%
	V	0.4%	0.34%	0.46%	1.06%	2.26%	5.09%	8.84%	15.16%	21.43%	28.50%
	UV	0.05%	0.11%	0.09%	0.57%	1.25%	2.89%	6.38%	12.15%	18.68%	26.44%

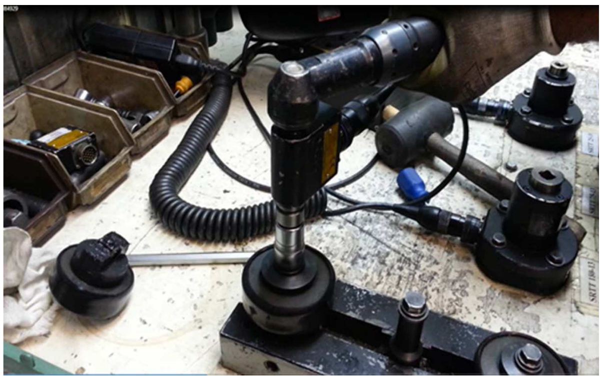

Figure 1. Different connection types of fastening twins (hard, semihard, and soft).

Figure 2. Torqometer for measurement of torque screws.

automotive industrial group discussed by Ayoubi et al. [40]. In this case, three different connection types of fastening twins, which are hard, semihard, and soft, are used. Figure 1 illustrates these connection types. Fixed values of torque are set to be measured by torqometer (see Figure 2) on the three connection types. Magnitudes of torque measured on the three types of connection are correlated because of the measurements by the same torqometer. Hence, it can be modeled using three-variate simple linear profiles. Table 10 shows 10 samples obtained from the process, all of

Table 9. The results (accuracy percent) of simultaneous shifts in the intercept, slope, and the standard deviation of the first and second profiles ($\rho = 0.5$).

		Intercept shifts from β_{01} to $\beta_{01}+\lambda_0\sigma_1$ in the first profile and β_{02} to $\beta_{02}+\lambda_0\sigma_2$ in the second profile									
Proposed control chart	λ_0	**0.2**	**0.4**	**0.6**	**0.8**	**1**	**1.2**	**1.4**	**1.6**	**1.8**	**2**
Max-MEWMA	U	75.75%	91.34%	92.04%	87.45%	77.99%	63.54%	43.40%	37.36%	24.46%	17.19%
	V	21.91%	5.40%	2.67%	2.39%	3.34%	3.69%	4.75%	5.96%	6.65%	9.94%
	UV	2.34%	3.26%	5.29%	10.16%	18.68%	32.77%	51.86%	56.67%	68.89%	72.87%
Max-MCUSAM	U	99.79%	99.94%	99.86%	99.46%	98.81%	96.96%	92.55%	85.56%	76. 36%	68.73%
	V	0.13%	0%	0%	0.05%	0.01%	0.01%	0%	0.01%	0.03%	0%
	UV	0.09%	0.06%	0.14%	0.49%	1.18%	3.02%	7.45%	14.42%	23.61%	31.27%
		Standard deviation shifts from σ_1 to $\gamma\sigma_1$ and σ_2 to $\gamma\sigma_2$									
Proposed control chart	γ	**1.1**	**1.2**	**1.3**	**1.4**	**1.5**	**1.6**	**1.7**	**1.8**	**1.9**	**2**
Max-MEWMA	U	22.04%	4.51%	0.98%	0.16%	0.04%	0.01%	0%	0%	0%	0%
	V	73.60%	89.02%	88.50%	82.04%	67.14%	47.66%	28.08%	13.85%	6.75%	3.30%
	UV	4.36%	6.46%	10.53%	17.80%	32.82%	52.32%	71.92%	86.15%	93.25%	96.70%
Max-MCUSAM	U	89.38%	29.64%	7.35%	2.59%	1.09%	0.66%	0.4 %	0.21%	0.08%	0.03%
	V	10.10%	66.50%	87.05%	89.75%	89.25%	87.99%	84.00%	80.53%	77.08%	74.06%
	UV	0.53%	3.86%	5.60%	7.66%	9.66%	11.35%	15.60%	19.26 %	22.85%	25.91%
		Slope shifts from β_{11} to $\beta_{11}+\lambda_1\sigma_1$ in the first profile and β_{12} to $\beta_{12}+\lambda_1\sigma_2$ in the second profile									
Proposed control chart	λ_1	**0.025**	**0.05**	**0.075**	**0.1**	**0.125**	**0.15**	**0.175**	**0.2**	**0.225**	**0.25**
Max-MEWMA	U	65.46%	83.85%	91.43%	92.61%	90.76%	87.06%	80.71%	71.38%	59.7 8%	48.13%
	V	32.62%	13.43%	4.91%	2.99%	2.62%	2.69%	3.04%	3.00%	4.3 9%	4.56%
	UV	1.91%	2.73%	3.66%	4.40%	6.61%	10.25%	16.25%	25.62 %	35.88%	47.31%
Max-MCUSAM	U	99.81%	99.96%	99.94%	99.96%	99.68%	99.52%	98.94%	97.58%	96. 295	92.74%
	V	0.13%	0.03%	0.04%	0.01%	0.01%	0.04%	0.01%	0.01%	0%	0.01%
	UV	0.06%	0.01%	0.03%	0.03%	0.031%	0.044%	1.05%	2.14%	3.71%	7.25%

which are in-control. Ayoubi et al. [41] used Jarque-Bera test to check normality assumption. The p-values of the Jarque-Bera tests for the first, second, and third profiles are 0.0813, 0.0497, and 0.0545, respectively. Considering confidence level of 0.95, the first and third profiles have no violations of the normality assumption. The confidence p-value of the normality test for the second profile is very close to the significant level of 0.05. Hence, they considered that the second profile error term also followed normal distribution roughly.

Ayoubi et al. [41] also used Pearson-correlation test to investigate correlation between profiles. They showed that the Pearson-correlation value was 0.9613 for the correlation between the measurements on hard and semihard connections with the p-value of 0.1592×10^{-27}. Between the hard and soft connections, correlation value is 0.9675 and the test p-value is equal to 0.0027×10^{-27}. Finally, semihard and soft connections have the correlation value of 0.9965 with the Pearson test p-value of zero. High magnitudes of correlation and p-values that are less than the significant level of 0.05 demonstrate that the correlations are significantly different from zero.

Another assumption for adequacy of regression equations is equality of error term variances in different levels of explanatory variable. To check this assumption, the relationship between the residuals and values of explanatory variable for three profiles are depicted as scatter plots in Figure 3 (a)-(c). As shown in the figures, the variances of error

Table 10. Data of torqometer calibration case study at Irankhodro Corporation [40]

Actual torque	Hard	Semihard	Soft	Hard	Semihard	Soft	Hard	Semihard	Soft
	First sample			**Second sample**			**Third sample**		
20	20.83	19.77	19.56	20.25	20.416	19.41	20.89	20.599	19.40
25	25.09	22.046	21.89	24.28	23.02	21.44	25.47	22.92	21.623
30	30.9	25.64	26.954	32.5	26.72	25.616	31.7	25.86	26.057
35	34.65	32.23	32.58	35.1	32.22	32.51	36.71	32.11	31.84
40	40.38	39.78	39.35	40.13	39.58	40.04	40.5	39.95	39.91
	Fourth sample			**Fifth sample**			**Sixth sample**		
20	21.16	20.40	19.42	20.07	20.36	19.30	20.66	20.49	19.25
25	25.34	22.835	21.38	26.11	22.35	21.56	25.43	23.04	22.22
30	30.50	25.90	26.09	29.99	26.93	25.51	32.73	25.73	26.65
35	33.8	32.30	32.60	36.90	32.10	32.74	34.30	32.00	32.65
40	40.20	39.16	40.80	41.10	39.68	40.34	40.20	39.33	40.20
	Seventh sample			**Eighth sample**			**Ninth sample**		
20	21.40	20.76	19.33	20.99	20.66	19.12	20.73	20.58	19.85
25	25.38	22.93	22.33	25.40	22.59	22.49	26.17	23.10	21.95
30	31.80	26.47	26.58	30.43	26.50	26.91	31.32	25.88	25.73
35	35.00	32.20	32.33	36.70	32.30	31.90	35.80	32.44	32.60
40	40.93	39.98	39.25	40.84	39.15	39.87	40.33	39.29	39.99
				Tenth sample					
20				20.30	20.49	19.48			
25				26.39	22.70	21.42			
30				32.58	25.93	25.79			
35				35.10	32.10	32.23			
40				40.20	39.73	40.02			

terms in each profile are equal in different levels of explanatory variable. In other words, there is no significant difference among variances of error terms in each profile under different levels of explanatory variable.

Finally, to check for independency of response variables of each profile over time, we use run chart and plot the mean of residuals in each profile for each sample versus time. The results are illustrated in Figure 4 (a)-(c) for the first, second, and third equations, respectively. As it is clear from the figures, the mean of residuals is independent over time for all equations of multivariate simple linear regression profile. In other words, there is no autocorrelation between profiles over time.

An in-control model fitted with the stable data with fixed x values of 20, 25, 30, 35, and 40 is as follows:

$$y_1 = 1.0696 + 0.9881x + \varepsilon_1,$$

$$y_2 = -0.3758 + 0.9534x + \varepsilon_2,$$

$$y_3 = -3.0574 + 1.0340x + \varepsilon_3,$$

where $(\varepsilon_1, \varepsilon_2, \varepsilon_3\ )$ is a multivariate normal random vector with mean vector zero and covariance matrix of:

$$\hat{\mathbf{\Sigma}} = \begin{pmatrix} 0.8514 & -0.5728 & -0.4667 \\ -0.5728 & 4.0003 & 3.6758 \\ -0.4667 & 3.6758 & 3.6971 \end{pmatrix}.$$

We compute the in-control Max-MEWMA, Max-MCUSUM, and ELRT statistics corresponding to samples 1-9 and then generate 6 samples with a sustained shift in the intercept of the first profile from $\beta_{01} = 1.0696$ to $\beta_{01} = 1.4$ from sample 10 and compute the statistics of the proposed control charts. The proposed control charts are presented in Figures 5 and 6 and ELR control chart is presented in Figure 7. In all of the control chart schemes, the upper control limit is chosen to achieve an in-control ARL of 200. The upper control limits for Max-MEWMA, Max-MCUSUM, and ELRT control charts are set equal to 2.96, 5.29, and 4.25, respectively, through simulation runs. The Max-MEWMA control chart signals in the three samples after the occurrence of shift (12th sample). In the Max-MCUSUM, the shift is detected in the 13th sample and ELRT control chart signals in the 14th sample. Hence, Max-MEWMA control chart performs better than Max-MCUSUM and ELRT control charts in detecting shifts in the intercept of the first profile in the real case. In addition, the diagnosing procedure of the proposed control charts shows that the process mean is changed.

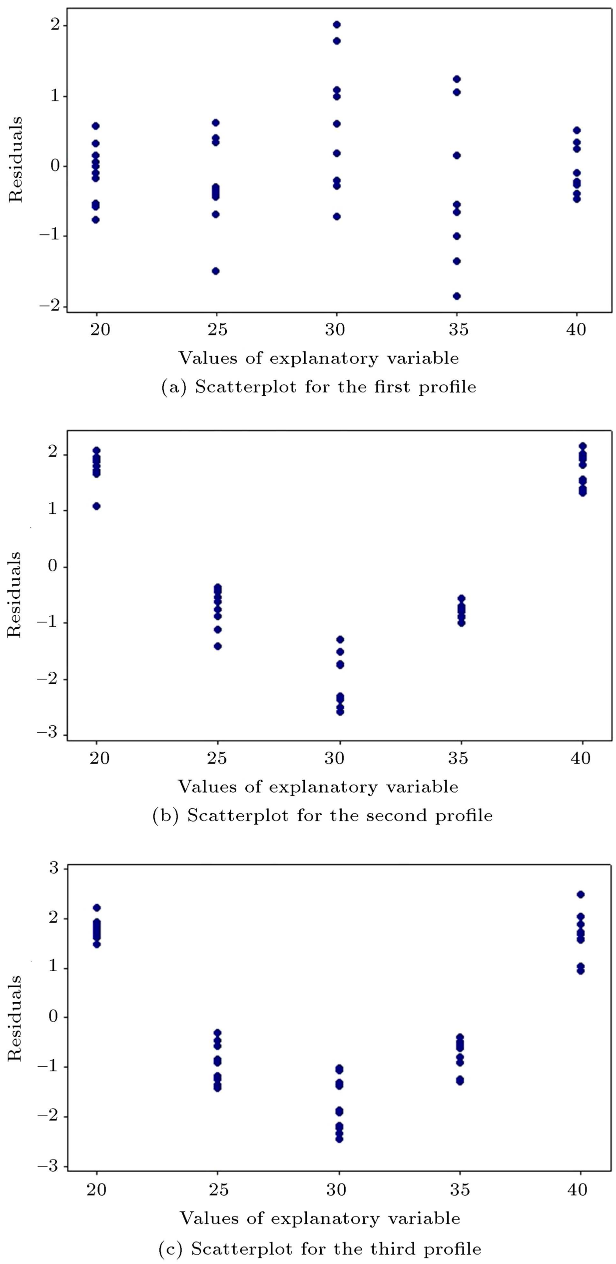

Figure 3. Plot of residuals versus values of explanatory variable for three profiles in the real-case data.

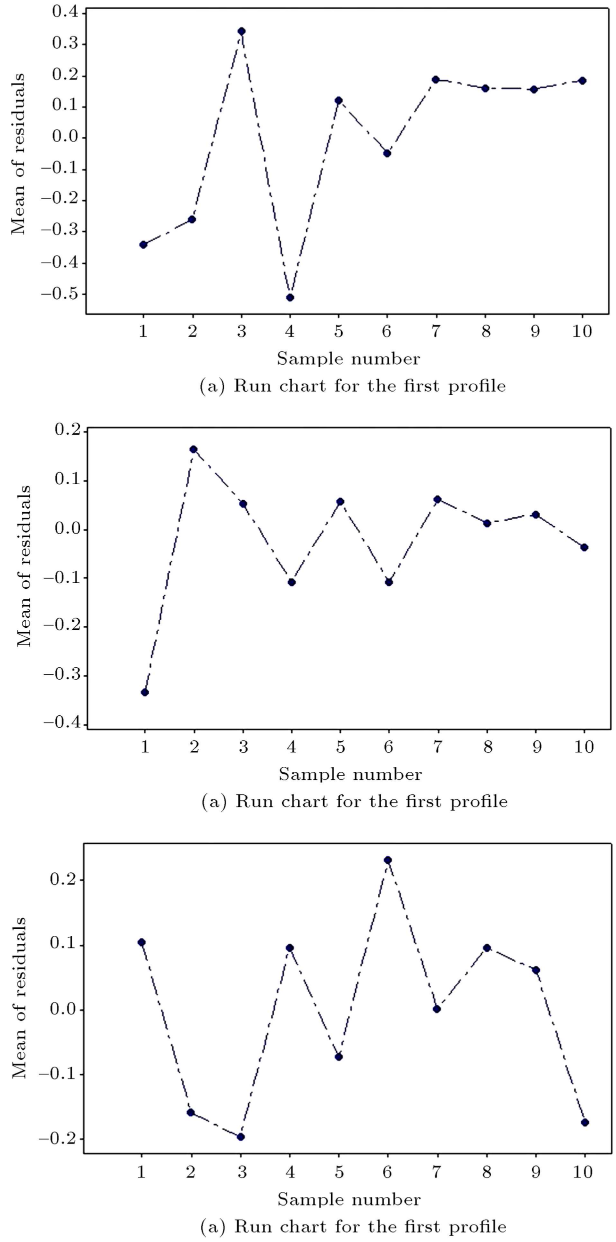

Figure 4. Independency of error terms over time for real-case data.

To investigate the performance of control charts in detecting shifts in standard deviation, we first generate 10 in-control multivariate simple linear profiles with the above-mentioned relationships. From the 11th sample, we generate out-of-control data, where the value of σ_3 shifts from 1.9227 to 2.1. The control charts based on the proposed methods and ELRT control chart are presented in Figures 8-10. The Max-MEWMA control chart signals in the 5th sample after the occurrence of shift (15th sample) and ELRT control chart signals in the 18th sample. The Max-MCUSUM control chart does not detect shift in the standard deviation based on the samples investigated. Not that, the diagnosing

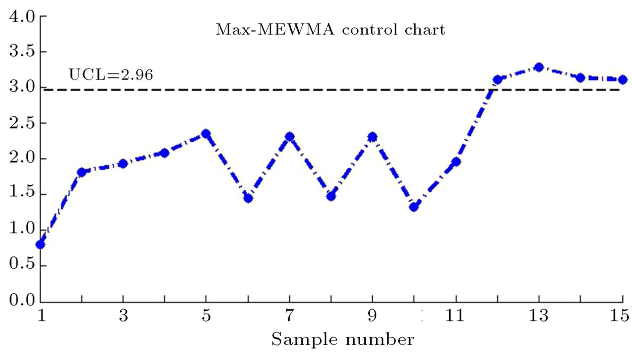

Figure 5. Max-MEWMA control chart for the calibration application data under shift from $\beta_{01} = 1.0696$ to $\beta_{01} = 1.4$ at the 10th sample.

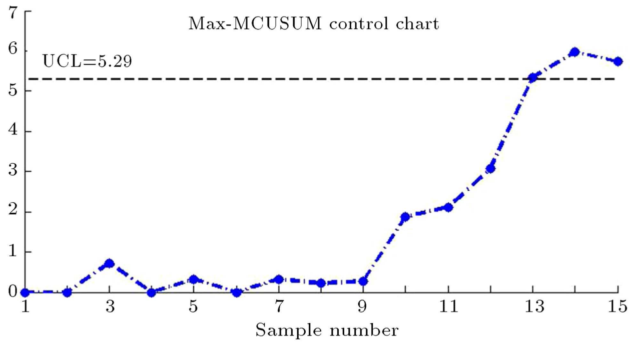

Figure 6. Max-MCUSUM control chart for the calibration application data under shift from $\beta_{01} = 1.0696$ to $\beta_{01} = 1.4$ at the 10th sample.

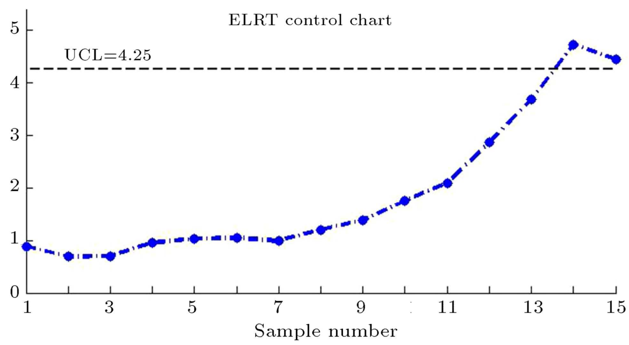

Figure 7. ELRT control chart for the calibration application data under shift from $\beta_{01} = 1.0696$ to $\beta_{01} = 1.4$ at the 10th sample.

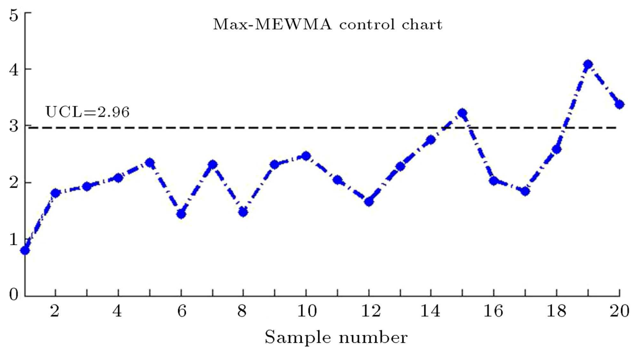

Figure 8. Max-MEWMA control chart for the calibration application data under shift from $\sigma_3 = 1.9227$ to $\sigma_3 = 2.1$ at the 11th sample.

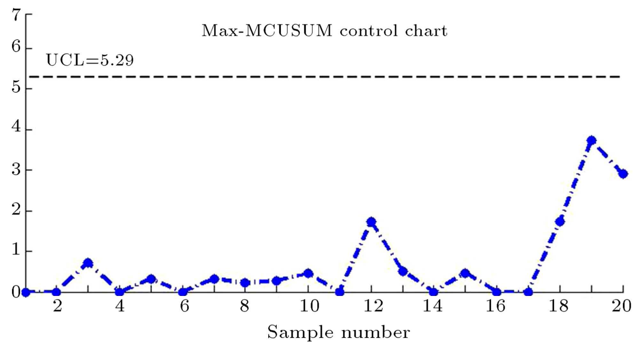

Figure 9. Max-MEWMA control chart for the calibration application data under shift from $\sigma_3 = 1.9227$ to $\sigma_3 = 2.1$ at the 11th sample.

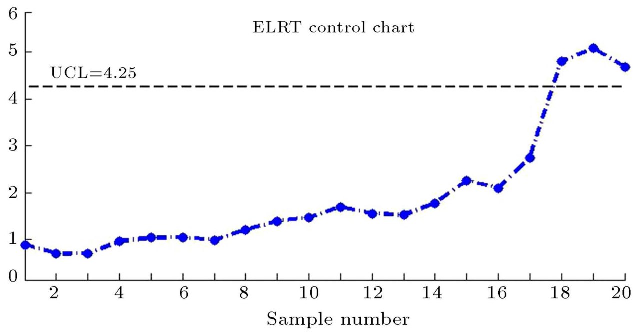

Figure 10. ELRT control chart for the calibration application data under shift from $\sigma_3 = 1.9227$ to $\sigma_3 = 2.1$ at the 11th sample.

procedure of Max-MEWMA control chart shows that the variation of the process is changed.

8. Conclusions and future research

In this paper, we developed two control charts including Max-MEWMA and Max-MCUSUM to simultaneously monitor mean vector and covariance matrix in multivariate multiple linear regression profiles in Phase II. The two proposed control charts had also the potential for diagnosing purpose. The performance of each control chart in detecting out-of-control states was investigated through simulation studies in terms of ARL and SDRL criteria. Simulation studies showed that the Max-MEWMA and the Max-MCUSUM control schemes performed slightly better than the ELRT control chart in detecting sustained shifts in the intercept and slope of multivariate linear regression profiles. Also, in detecting shift in the elements of variance-covariance matrix, Max-MEWMA control chart was better than the Max-MCUSUM and ELRT control charts. We also evaluated the performance of the control charts for diagnosing purpose. Results showed that the diagnosing procedure in Max-MEWMA control chart under small and large shifts in the intercept, slope, and standard deviation performed satisfactorily. Furthermore, the diagnosing procedure performance of the Max-MCUSUM control chart under shifts in intercept, slope, and standard deviation was satisfactory. Finally, we showed the use of the proposed control charts in a real calibration case in the automotive industry. For future research, we recommend developing a method to diagnose the parameters responsible for out-of-control signals. Furthermore, developing a multivariate self-starting control chart for simultaneous monitoring of mean vector and covariance matrix in multivariate multiple linear regression profiles can be a fruitful area.

Acknowledgment

The authors are grateful to the anonymous referees for precious comments, which led to improvement of the paper.

References

1. Kang, L. and Albin, S.L. "On-line monitoring when the process yields a linear profile". *Journal of Quality Technology*, **32**(4), pp. 418-426 (2000).
2. Mahmoud, M.A. and Woodall, W.H. "Phase I analysis of linear profiles with calibration applications". *Technometrics*, **46**(4), pp. 380-391 (2004).
3. Woodall, W.H., Spitzner, D.J., Montgomery, D.C. and Gupta, S. "Using control charts to monitor process and product quality profiles", *Journal of Quality Technology*, **36**(3), pp. 309-320 (2004).
4. Wang, K. and Tsung, F. "Using profile monitoring techniques for a data-rich environment with huge sample size", *Quality and Reliability Engineering International*, **21**(7), pp. 677-688 (2005).
5. Woodall, W.H. "Current research on profile monitoring", *Production*, **17**(3), pp. 420-425 (2007).
6. Zou, C., Tsung, F. and Wang, Z. "Monitoring general linear profiles using multivariate exponentially weighted moving average schemes", *Technometrics*,**49**(4), pp. 395-408 (2007).
7. Amiri, A., Jensen, W.A. and Kazemzadeh, R.B. "A case study on monitoring polynomial profiles in the automotive industry", *Quality and Reliability Engineering International*, **26**(5), pp. 509-520 (2010).
8. Kim, K., Mahmoud, M.A. and Woodall, W.H. "On the monitoring of linear profiles", *Journal of Quality Technology*, **35**(3), pp. 317-328 (2003).
9. Keshtelia, R.N., Kazemzadeha, R.B., Amirib, A. and Noorossanac, R. "Developing functional process capability indices for simple linear profile", *Scientia Iranica*, **21**(3), pp. 1044-1050 (2014).
10. Noorossana, R. and Ayoubi, M. "Profile monitoring using nonparametric bootstrap T2 control chart", *Communications in Statistics-Simulation and Computation*, **41**(3), pp. 302-315 (2012).
11. Chuang, S.C, Hung, Y.C., Tsai, W.C. and Yang, S.F. "A framework for nonparametric profile monitoring", *Computers and Industrial Engineering*, **64**(1), pp. 482-491 (2013).
12. Mahmoud, M.A., Parker, P.A., Woodall, W.H. and Hawkins, D.M. "A change point method for linear profile data", *Quality and Reliability Engineering International*, **23**(2), pp. 247-268 (2007).
13. Kazemzadeh, R.B., Noorossana, R and Amiri, A. "Phase I monitoring of polynomial profiles", *Communications in Statistics-Theory and Methods*, **37**(10), pp. 1671-1686 (2008).
14. Kazemzadeh, R.B., Noorossana, R., and Amiri, A. "Phase II Monitoring of Autocorrelated Polynomial Profiles in AR(1) Processes", *Scientia Iranica,* **17**(1), pp. 12-24 (2010).
15. Amiri, A., Eyvazian, M., Zou, C. and Noorossana, R. "A parameters reduction method for monitoring multiple linear regression profiles", *The International Journal of Advanced Manufacturing Technology*, **58**(5-8), pp. 621-629 (2012).
16. Wang, FK. "Supplier selection for multiple linear profiles with one-sided specifications", *Quality and Reliability Engineering International*, published online. (2014)
17. Amiri, A., Saghaei, A., Mohseni, M. and Zerehsaz, Y. "Diagnosis aids in multivariate multiple linear regression profiles monitoring", *Communications in Statistics-Theory and Methods*, **43**(14), pp. 3057-3079 (2014).
18. Noorossana, R., Eyvazian, M. and Vaghefi, A. "Phase II monitoring of multivariate simple linear profiles", *Computers & Industrial Engineering*, **58**(4), pp. 563-570 (2010a).
19. Noorossana, R., Eyvazian, M., Amiri, A. and Mahmoud, M.A. "Statistical monitoring of multivariate multiple linear regression profiles in phase I with calibration application", *Quality and Reliability Engineering International*, **26**(3), pp. 291-303 (2010b).
20. Zhang, J., Ren, H., Yao, R., Zou, C. and Wang, Z. "Phase I analysis of multivariate profiles based on regression adjustment", *Computers & Industrial Engineering*, **85**, pp. 132-144 (2015).
21. Eyvazian, M., Noorossana, R., Saghaei, A. and Amiri, A. "Phase II monitoring of multivariate multiple linear regression profiles", *Quality and Reliability Engineering International*, **27**(3), pp. 281-296 (2011).
22. Khoo, M.B., Teh, S.Y. and Wu, Z. "Monitoring process mean and variability with one double EWMA chart", *Communications in Statistics-Theory and Methods,* **39**(20), pp. 3678-3694 (2010).
23. Zhang, J., Zou, C. and Wang, Z. "A control chart based on likelihood ratio test for monitoring process mean and variability", *Quality and Reliability Engineering International*, **26**(1), pp. 63-73 (2010a).
24. Guh, RS. "Simultaneous process mean and variance monitoring using artificial neural networks", *Computers & Industrial Engineering*, **58**(4), pp. 739-753 (2010).
25. Ostadsharif Memar, A. and Niaki, STA. "The Max EWMAMS control chart for joint monitoring of process mean and variance with individual observations", *Quality and Reliability Engineering International*, **27**(4), pp. 499-514 (2011).
26. Teh, S.Y., Khoo, M.B. and Wu, Z. "Monitoring process mean and variance with a single generally weighted moving average chart", *Communications in Statistics-Theory and Methods,* **41**(12), pp. 2221-2241 (2012).

27. Sheu, S.H., Huang, C.J. and Hsu, T.S. "Maximum chi-square generally weighted moving average control chart for monitoring process mean and variability", *Communications in Statistics-Theory and Methods*, **42**(23), pp. 4323-4341 (2013).

28. Haq, A., Brown, J. and Moltchanova, E. "An improved maximum exponentially weighted moving average control chart for monitoring process mean and variability", *Quality and Reliability Engineering International*, **31**(2), pp. 265-290 (2015).

29. Prajapati, D.R. and Singh, S. "Monitoring of process mean and variance simultaneously by joint and R chart for serial correlation", *International Journal of Productivity and Quality Management*, **16**(1), pp. 70-91 (2015).

30. Chen, G., Cheng, S.W. and Xie, H. "A new multivariate control chart for monitoring both location and dispersion", *Communications in Statistics-Simulation and Computation*, **34**(1), pp. 203-217 (2005).

31. Cheng, S.W. and Thaga, K. "Multivariate max-CUSUM chart", *Quality Technology and Quantitative Management*, **2**(2), pp. 221-235 (2005).

32. Zhang, J., Li, Z. and Wang, Z. "A multivariate control chart for simultaneously monitoring process mean and variability", *Computational Statistics and Data Analysis*, **54**(10), pp. 2244-2252 (2010).

33. Wang, K., Yeh, A.B. and Li, B. "Simultaneous monitoring of process mean vector and covariance matrix via penalized likelihood estimation", *Computational Statistics & Data Analysis*, **78**, pp. 206-217 (2014).

34. Khoo, M.B. "A new bivariate control chart to monitor the multivariate process mean and variance simultaneously", *Quality Engineering*, **17**(1), pp. 109-118 (2004).

35. Hawkins, D.M. and Maboudou-Tchao, E.M. "Multivariate exponentially weighted moving covariance matrix", *Technometrics*, **50**(2), pp. 155-166 (2008).

36. Ramos, P.F., Morais, M.C., Pacheco, A. and Schmid, W. "Misleading signals in simultaneous schemes for the mean vector and covariance matrix of a bivariate process", *In Recent Developments in Modeling and Applications in Statistics*. Springer Berlin Heidelberg, pp. 225-235 (2013).

37. Pirhooshyaran, M. and Niaki, STA. "A double-max MEWMA scheme for simultaneous monitoring and fault isolation of multivariate multistage autocorrelated processes based on novel reduced-dimension statistics", *Journal of Process Control*, **29**, pp. 11-22 (2015).

38. McCracken, A.K. and Chakraborti, S. "Control charts for joint monitoring of mean and variance: an overview", *Quality Technology and Quantitative Management,* **10**(1), pp. 17-36 (2013).

39. Healy, J.D. "A note on multivariate CUSUM procedures", *Technometrics*, **29**(4), pp. 409-412 (1987).

40. Ayoubi, M., Kazemzadeh, R.B. and Noorossana, R. "Estimating multivariate linear profiles change point with a monotonic change in the mean of response variables", *The International Journal of Advanced Manufacturing Technology*, **75**(9-12), pp. 1537-1556 (2014).

41. Ayoubi, M., Kazemzadeh, R.B. and Noorossana, R. "Change point estimation in the mean of multivariate linear profiles with no change type assumption via dynamic linear model", *Quality and Reliability Engineering International*, **32**(2), pp. 403-433 (2015).

Appendix A

The likelihood ratio for MCUSUM control chart under multivariate normal distribution and shift in mean vector is calculated by Eq. (A.1) as shown in Box A.I.

Taking natural logarithms as follows:

$$\log\frac{f_b(x_k)}{f_g(x_k)} = -0.5(\hat{\boldsymbol{\beta}}_k-\boldsymbol{\beta}_b)\Sigma^{-1}_{\hat{\boldsymbol{\beta}}_k}(\hat{\boldsymbol{\beta}}_k-\boldsymbol{\beta}_b)' +0.5(\hat{\boldsymbol{\beta}}_k-\boldsymbol{\beta}_g)\Sigma^{-1}_{\hat{\boldsymbol{\beta}}_k}(\hat{\boldsymbol{\beta}}_k-\boldsymbol{\beta}_g)', \tag{A.2}$$

after simplifying, we have:

$$\begin{aligned}\log\frac{f_b(x_k)}{f_g(x_k)} &= -0.5\hat{\boldsymbol{\beta}}_k\Sigma^{-1}_{\hat{\boldsymbol{\beta}}_k}\hat{\boldsymbol{\beta}}'_k+0.5\hat{\boldsymbol{\beta}}_k\Sigma^{-1}_{\hat{\boldsymbol{\beta}}_k}\boldsymbol{\beta}'_b \\ &\quad +0.5\boldsymbol{\beta}_b\Sigma^{-1}_{\hat{\boldsymbol{\beta}}_k}\hat{\boldsymbol{\beta}}'_k-0.5\boldsymbol{\beta}_b\Sigma^{-1}_{\hat{\boldsymbol{\beta}}_k}\hat{\boldsymbol{\beta}}'_b \\ &\quad +0.5\hat{\boldsymbol{\beta}}_k\Sigma^{-1}_{\hat{\boldsymbol{\beta}}_k}\hat{\boldsymbol{\beta}}'_k-0.5\hat{\boldsymbol{\beta}}_k\Sigma^{-1}_{\hat{\boldsymbol{\beta}}_k}\boldsymbol{\beta}'_g \\ &\quad -0.5\boldsymbol{\beta}_g\Sigma^{-1}_{\hat{\boldsymbol{\beta}}_k}\hat{\boldsymbol{\beta}}'_k+0.5\boldsymbol{\beta}_g\Sigma^{-1}_{\hat{\boldsymbol{\beta}}_k}\hat{\boldsymbol{\beta}}'_g \\ &= +0.5\hat{\boldsymbol{\beta}}_k\Sigma^{-1}_{\hat{\boldsymbol{\beta}}_k}(\boldsymbol{\beta}_b-\boldsymbol{\beta}_g)' \\ &\quad +0.5(\boldsymbol{\beta}_b-\boldsymbol{\beta}_g)\Sigma^{-1}_{\hat{\boldsymbol{\beta}}_k}\hat{\boldsymbol{\beta}}'_k \\ &\quad -0.5(\boldsymbol{\beta}_b-\boldsymbol{\beta}_g)\Sigma^{-1}_{\hat{\boldsymbol{\beta}}_k}(\boldsymbol{\beta}_b-\boldsymbol{\beta}_g) \\ &= (\boldsymbol{\beta}_b-\boldsymbol{\beta}_g)\Sigma^{-1}_{\hat{\boldsymbol{\beta}}_k}\hat{\boldsymbol{\beta}}'_k \\ &\quad -0.5(\boldsymbol{\beta}_b+\boldsymbol{\beta}_g)\Sigma^{-1}_{\hat{\boldsymbol{\beta}}_k}(\boldsymbol{\beta}_b-\boldsymbol{\beta}_g)', \end{aligned} \tag{A.3}$$

and equivalently we have:

$$\log\frac{f_b(x_k)}{f_g(x_k)} =(\boldsymbol{\beta}_b-\boldsymbol{\beta}_g)\Sigma^{-1}_{\hat{\boldsymbol{\beta}}_k}\hat{\boldsymbol{\beta}}'_k-0.5(\boldsymbol{\beta}_b+\boldsymbol{\beta}_g) \Sigma^{-1}_{\hat{\boldsymbol{\beta}}_k}(\boldsymbol{\beta}_b-\boldsymbol{\beta}_g)'. \tag{A.4}$$

$$\frac{f_b(x_k)}{f_g(x_k)} = \frac{(2\pi)^{-p/2}\left|\Sigma_{\hat{\boldsymbol{\beta}}_k}^{-1}\right|^{-1/2}\exp(-0.5(\hat{\boldsymbol{\beta}}_k-\boldsymbol{\beta}_b)\Sigma_{\hat{\boldsymbol{\beta}}_k}^{-1}(\hat{\boldsymbol{\beta}}_k-\boldsymbol{\beta}_b)')}{(2\pi)^{-p/2}\left|\Sigma_{\hat{\boldsymbol{\beta}}_k}^{-1}\right|^{-1/2}\exp(-0.5(\hat{\boldsymbol{\beta}}_k-\boldsymbol{\beta}_g)\Sigma_{\hat{\boldsymbol{\beta}}_k}^{-1}(\hat{\boldsymbol{\beta}}_k-\boldsymbol{\beta}_g)')} = \frac{\exp(-0.5(\hat{\boldsymbol{\beta}}_k-\boldsymbol{\beta}_b)\Sigma_{\hat{\boldsymbol{\beta}}_k}^{-1}(\hat{\boldsymbol{\beta}}_k-\boldsymbol{\beta}_b)')}{\exp(-0.5(\hat{\boldsymbol{\beta}}_k-\boldsymbol{\beta}_g)\Sigma_{\hat{\boldsymbol{\beta}}_k}^{-1}(\hat{\boldsymbol{\beta}}_k-\boldsymbol{\beta}_g)')}. \quad \text{(A.1)}$$

Box A.I

$$\frac{f_b(x_k)}{f_g(x_k)} = \frac{(2\pi)^{-p/2}\left|b\Sigma_{\hat{\boldsymbol{\beta}}_k}\right|^{-1/2}\exp(-0.5(\hat{\boldsymbol{\beta}}_k-\boldsymbol{\beta}_g)(b\Sigma_{\hat{\boldsymbol{\beta}}_k})^{-1}(\hat{\boldsymbol{\beta}}_k-\boldsymbol{\beta}_g)')}{(2\pi)^{-p/2}\left|\Sigma_{\hat{\boldsymbol{\beta}}_k}\right|^{-1/2}\exp(-0.5(\hat{\boldsymbol{\beta}}_k-\boldsymbol{\beta}_g)\Sigma_{\hat{\boldsymbol{\beta}}_k}^{-1}(\hat{\boldsymbol{\beta}}_k-\boldsymbol{\beta}_g)')}. \quad \text{(B.1)}$$

Box B.I

Appendix B

The likelihood ratio for MCUSUM control chart under multivariate normal distribution and shift in covariance matrix is obtained by Eq. (B.1) as shown in Box B.I. After simplifying, we have:

$$\frac{f_b(x_k)}{f_g(x_k)} = b^{-1/2}\exp[-0.5(\hat{\boldsymbol{\beta}}_k-\boldsymbol{\beta}_g)$$
$$\Sigma_{\hat{\boldsymbol{\beta}}_k}^{-1}(\hat{\boldsymbol{\beta}}_k-\boldsymbol{\beta}_g)'(\frac{1}{b}-1)], \quad \text{(B.2)}$$

taking natural logarithms:

$$\log\frac{f_b(x_k)}{f_g(x_k)} = \frac{-1}{2}\log b + 0.5(\hat{\boldsymbol{\beta}}_k-\boldsymbol{\beta}_g)$$
$$\Sigma_{\hat{\boldsymbol{\beta}}_k}^{-1}(\hat{\boldsymbol{\beta}}_k-\boldsymbol{\beta}_g)'(1-\frac{1}{b}). \quad \text{(B.3)}$$

Biographies

Reza Ghashghaei is an MSc student of Industrial Engineering at Shahed University in Iran. His research interests are statistical quality control and measurement error.

Amirhossein Amiri is an Associate Professor at Shahed University in Iran. He holds BS, MS, and PhD degree in Industrial Engineering from Khajeh Nasir University of Technology, Iran University of Science and Technology, and Tarbiat Modares University in Iran, respectively. He is now Vice Chancellor of Education in Faculty of Engineering at Shahed University in Iran and a member of the Iranian Statistical Association. His research interests are statistical quality control, profile monitoring, and Six Sigma. He has published many papers in the area of statistical process control in high-quality international journals such as Quality and Reliability Engineering International, Communications in Statistics, Computers and Industrial Engineering, Journal of Statistical Computation and Simulation, Soft Computing, etc. He has also published a book with John Wiley and Sons in 2011 entitled Statistical Analysis of Profile Monitoring.